

The nature of the Schönberg–Chandrasekhar limit

Janusz Ziółkowski^{*} and Andrzej A. Zdziarski^{*}

Nicolaus Copernicus Astronomical Center, Polish Academy of Sciences, Bartycka 18, PL-00-716 Warszawa, Poland

6 October 2020

ABSTRACT

We present a comprehensive description of the Schönberg–Chandrasekhar (S–C) transition, which is an acceleration of the stellar evolution from the nuclear to the thermal time scales occurring when the fractional mass of the helium core reaches a critical value, about 0.1. It occurs in the 1.4 to 7 M_{\odot} mass range due to impossibility of maintaining the thermal equilibrium after the nuclear energy sources in the core disappear. We present the distributions of the hydrogen abundance, the energy generation rate and the temperature for stars crossing that limit. We confirm that a sharp S–C limit is present for strictly isothermal cores, but it is much smoother for real stars. The way the boundary of the core is defined is important for the picture of this transition. With a strict definition of the core as the region where the helium abundance is close to null, it occurs in an extended range of the fractional core mass of roughly 0.03 to 0.11. The cause of that is a gradual core contraction causing a correspondingly gradual loss of the core isothermality with the increasing core mass. On the other hand, when using definitions allowing for some H abundance in the core, the S–C transition is found to be sharper, at the fractional core mass of between about 0.07 and 0.11. Still, it is more a smooth transition than a sharp limit. We have also searched for specific signatures of that transition, and found that it is associated with the stellar radius first decreasing and then increasing again. We have considered whether the S–C limit can be used as a diagnostic constraining the evolutionary status of accreting X-ray binaries, but found such uses unfounded.

Key words: stars: general – stars: evolution – stars: interiors – Hertzsprung–Russell and colour-magnitude diagrams

1 INTRODUCTION

The concept of the Schönberg–Chandrasekhar (hereinafter S–C) limit is one of the classic results of the early stellar evolution theory. Its history started with the suggestion by Gamov (1938) that a helium core left after the hydrogen exhaustion in the central part of a star should become isothermal owing to the lack of the energy sources within the core. Next, Henrich & Chandrasekhar (1941) calculated models containing such isothermal cores but not consisting of He; they constructed homogeneous models in which chemical composition was the same for the core and the envelope. They found that it was possible to construct a model if the relative mass of the isothermal core, $q_c \equiv M_c/M$, was less than about 0.38. In a later paper, Schönberg & Chandrasekhar (1942) constructed more physically realistic models in which the configuration was composed of a He core and an H-rich envelope. Such configurations are a natural outcome of the core H-burning phase. They found the limit of

$$q_c \lesssim 0.37 \left(\frac{\mu_{\text{env}}}{\mu_c} \right)^2, \quad (1)$$

which has become known as the S–C limit. Here, μ_{env} and μ_c are the mean molecular weights of the envelope and core, respectively. For $\mu_{\text{env}} = 0.6$ (about cosmic composition) and $\mu_c = 1.3$ (He dominated), $q_c \approx 0.08$. Above this core mass, the core collapses. This leads to an acceleration of the evolution, from a nuclear to a thermal time-scale. This also represents the onset of the Hertzsprung gap.

Soon, it became clear that the S–C limit cannot be universal. Models of Schönberg & Chandrasekhar (1942) were simplified and, in particular, used the ideal gas equation of state. As noted by Hayashi, Hoshi & Sugimoto (1962), the He cores of stars with a total mass of $M \lesssim 1.3M_{\odot}$ become quickly degenerate, and then they remain isothermal even above the S–C limit. On the other hand, Cox & Giuli (1968) claimed that the cores (defined by the H abundance being relatively low) of stars with $M \gtrsim 6M_{\odot}$ are already heavier than the S–C limit already at the moment of the central hydrogen exhaustion. Some years later, Roth (1973) constructed models of stars after central H exhaustion. These were idealized in having strictly isothermal cores, but otherwise included all the relevant physics. Roth (1973) constructed evolutionary sequences following the growth of the core mass owing to H shell burning for several stellar masses in the 1 to 3 M_{\odot} range and confirmed that such idealized configurations had thermally stable solutions up to certain critical q_c (i.e. up to the S–C limit) and then had to jump discontinuously to another branch of thermally stable solution with a much smaller core radius (see, e.g., fig. 30.16 of Kippenhahn, Weigert & Weiss 2012). Roth (1973) also found that the S–C limit disappears for such idealized stars with $M \lesssim 1.4M_{\odot}$, as well as noted that the real stars would have to evolve through non-equilibrium models. Indeed, a very fast transition between stable models near the main sequence and near the giant branch does occur in the evolution of real stars, forming the Hertzsprung gap. The PhD thesis results of Roth (1973) are summarized in detail by Kippenhahn et al. (2012).

The S–C limit was later analysed by some other authors, though not much progress has been achieved with respect to the above results. Eggleton & Faulkner (1981) and Eggleton, Faulkner & Can-

^{*} E-mail: jz@camk.edu.pl, aaz@camk.edu.pl

non (1998) discussed whether the existence of the S–C limit could by itself explain the transformation of a star into a red giant after central hydrogen exhaustion. The answer was negative; the S–C limit can explain why the core has to contract but it cannot explain why the envelope has to simultaneously expand. Beech (1988) considered configurations similar to those discussed in the original Henrich & Chandrasekhar (1941) and Schönberg & Chandrasekhar (1942) papers. Beech (1988) demonstrated that it is possible to derive the S–C limit by approximating the star with a simplified composite model with an isothermal core surrounded by an $n = 1$ polytropic envelope. Beech (1988) found that the limiting relative mass of the isothermal core is 0.27 for a chemically homogeneous configuration and 0.10 for the configuration composed of a He core and H-rich envelope; the latter agrees with that found by Schönberg & Chandrasekhar (1942). The former differs from the result of Henrich & Chandrasekhar (1941), having 0.27 instead of 0.37. This is probably because an $n = 1$ polytrope (chosen for computational convenience) is a worse approximation of the envelope than the one with a more realistic $n = 3$ used by Henrich & Chandrasekhar (1941).

Eggleton et al. (1998) considered simple analytic two-polytrope models in which the core and envelope were approximated by $n = 5$ and 1 polytropes, respectively. They assumed a jump in the chemical composition between the core and the envelope. The size of this jump (namely the ratio, α , of the mean molecular weight of the gas in the core and in the envelope) was a free parameter of the model. They found that the S–C phenomenon is not present (i.e., the fractional core mass can be arbitrarily large) for $\alpha < 3$. For $\alpha = 3$, the S–C phenomenon abruptly appears and the value of the limit is $2/\pi \approx 0.64$, while the classical value is 0.10. The phenomenon is also present for all values of $\alpha > 3$. However, $\alpha \geq 3$ does not correspond to a typical case of a He core and a Population I envelope, where $\alpha = 2.2$. In the case of a carbon-oxygen core, $\alpha = 3.3$. Their unexpected result, namely the lack of the S–C phenomenon in the most typical case, appears to be due to the use of the $n = 5$ polytrope as an approximation for the core of the star, while the isothermal core formally corresponds to a polytrope with $n \rightarrow \infty$. Indeed, when using $n > 5$, Eggleton et al. (1998) found the S–C phenomenon at any α .

We note that at present we have tools to construct precise stellar models, and there is no longer a need to limit the study to models using polytropes and/or assuming the core to be isothermal. Here, we use an evolutionary code developed from that of Paczyński (1969, 1970) to study in detail the behaviour of stars in the 1 to 7 M_{\odot} mass range from the moment of their leaving the main sequence up to the moving to the giant branch. We search for signatures of the S–C limit, in particular the acceleration of the evolution. An issue we find to be crucial is the way the He core, and thus q_c , are defined. A possible option is to define the core as the region where He completely dominates the composition and the burning of hydrogen is negligible. This corresponds to the fractional H abundance of $X \lesssim 10^{-6}$. Such a definition is adopted, in particular, in our stellar evolution code. On the other hand, the S–C limit has been derived based on the pressure balance at a boundary between the core and the envelope. Obviously, such boundary has to have a H abundance intermediate between that of the envelope and of the hydrogen-less core interior. We have found that q_c corresponding to a given evolutionary phase strongly depends on the definition of q_c . If the strict definition (no hydrogen in the core) is adopted, the acceleration already starts at $q_c \approx 0.03$ and the core mass gradually increases while going through the formal S–C limit. With that strict definition, there is no S–C limit, but rather an extended S–C transition, with the core losing isothermality and collapsing over a relatively wide range of

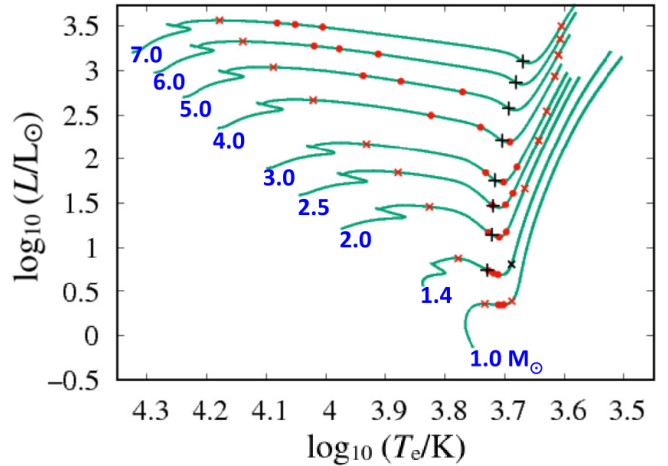


Figure 1. Evolutionary tracks in the H–R diagram (the luminosity vs. the effective surface temperature) for stars in the mass range of 1 to 7 M_{\odot} . The masses are marked at the beginning of each track. Red crosses (\times) show the points where $q_{c0} = 0.06$ (left) and 0.12 (right). The red dots show the points where $q_{c0} = 0.09, 0.095$ and 0.1 (from left to right). The black signs ($+$) correspond to the location of the kinks of the stellar radius as a function of time, shown in Fig. 6 below. The kinks visible to the left of those discussed above correspond to the exhaustion of H at the stellar centre, when the star leaves the main sequence.

q_c . On the other hand, if a less strict (but still physically justifiable) definition is adopted, then the S–C transition is sharper. Here, we use two such less strict definitions, namely q_{c1} corresponding to the radius at which the core switches from contracting to expanding, and q_{c2} corresponding to the radius where $X = 0.01$ is reached.

In our study, we also attempt to determine whether the S–C limit can be used to constrain the evolutionary status of a star in the absence of detailed spectroscopic information, especially in the case of donors of accreting X-ray binaries, in which case some specific S–C constraints were applied in the past.

In order to clarify these uncertainties about the meaning and nature of the S–C limit, we have constructed detailed evolutionary models of stars crossing that limit. We have studied the related evolutionary effects, and attempted to provide a detailed description of of the evolution, in particular with respect to evolutionary time and the core mass, and paying attention to the way the core is defined. We have also searched for any additional signatures of this crossing.

2 THE EVOLUTIONARY MODELS

We use the Warsaw stellar evolution code of Paczyński (1969, 1970), then developed by M. Kozłowski and R. Sienkiewicz. Its main current features and updates (e.g., the opacities, nuclear reaction rates and equation of state) are described by Pamyatnykh et al. (1998) and Ziółkowski (2005). Zdziarski et al. (2016), calibrated the code to reproduce the Sun at the solar age. This resulted in a H mass fraction of $X = 0.74$, a metallicity of $Z = 0.014$, and a mixing length parameter of 1.55 (adopting the version of the mixing theory of Paczyński 1969). Here, we use these values to follow evolution of stars in the mass range¹ of 1 to 7 M_{\odot} up to the advanced (with a luminosity of more than $10^3 L_{\odot}$) red giant branch.

¹ We have considered the evolution of an 8 M_{\odot} star, but for this mass the central He burning already takes place during the relevant evolutionary phase.

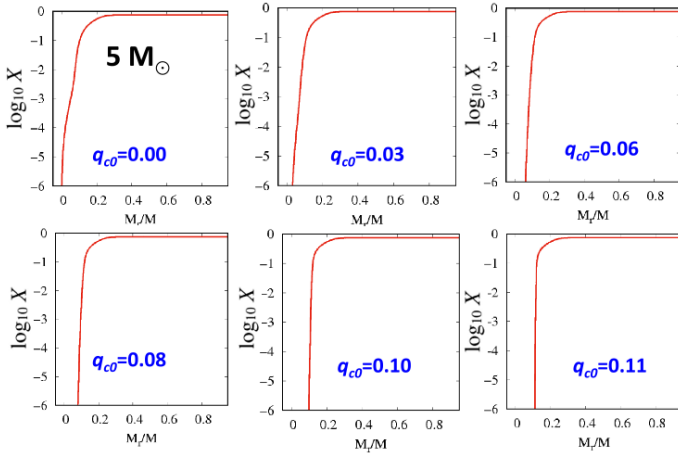


Figure 2. The H abundance vs. the ratio of the enclosed mass for a $5M_{\odot}$ star at 6 values of q_{c0} . We see that X increases gradually. This effect is especially pronounced for low q_{c0} . After the S–C transition, the core boundary becomes well defined.

The evolutionary tracks in the Hertzsprung–Russell (H–R) diagram are shown in Fig. 1. The transition through the S–C phase happens after hydrogen is exhausted at the stellar centre. This exhaustion corresponds to the second direction reversal (counting from the left-hand side) on the shown evolutionary tracks for $M \geq 1.4M_{\odot}$. At this point, the fractional core mass is null according to its strict definition, with an H abundance of $X \leq 10^{-6}$, which corresponds to its burning being completely negligible. Hereinafter, we denote the fractional mass of the core defined in this way by q_{c0} . Then, the minima of L correspond to the Hayashi line, at the transition from the subgiant to the giant branch, and they correspond to $q_{c0} \approx 0.11$.

As we have mentioned above, the H abundance increases with the enclosed mass rather gradually, especially before crossing the S–C phase. This is illustrated in Fig. 2, which shows the dependence of X on the (running) mass enclosed within a given radius, M_r , for a star with $5M_{\odot}$ at 6 values of q_{c0} . Thus, we see that the actual definition of the core boundary is quite fuzzy. Therefore, we define here two additional fractions. One is q_{c1} , corresponding to the radius at which the core switches from contracting to expanding. The other is q_{c2} , corresponding to the radius where $X = 0.01$. Another possible definition is the radius at which the energy flux generated in the nuclear reactions equals the gravitational energy flux (generated by core contraction, see Fig. 3). The M_c/M defined that way is generally close to q_{c1} (except when $q_{c0} = 0$).

Of course, the physical picture of stellar evolution of the star does not depend on the definition of q_c . However, as we show below, the picture of the S–C transition does depend on it. Namely, the rate of the stellar evolution as a function of q_c during that transition is quite different for different definitions, and then the transition covers different ranges of q_c .

In order to gain further insights into the structure of the core, we show in Fig. 3 the local luminosity (i.e., the total energy flux through the surface of a sphere of a given radius), L_r/L , as a function of the fractional mass enclosed, M_r/M , for a $5M_{\odot}$ star at different fractional masses of the core defined by q_{c0} . Here L is the total surface luminosity of the star. The green curve shows the gravitational energy flux (which is greater than 0 within the contracting core and less

than 0 during expansion). The blue curve shows the flux generated in the nuclear reactions. The red curve gives the net energy flux, being the sum of the previous two. The steeply rising parts of L_r on the first four panels correspond to the H shell burning, which generates most of the total energy. The energy generated by the collapsing core is shown by the rising part of L_r below the H-burning shell. We see that the shell remains around $M_r/M \approx 0.1$ for q_{c0} in the 0.03–0.10 range, i.e., the mass within the shell can be much higher than that of the core defined by the completely negligible H burning. The declining part of L_r corresponds to the expanding envelope. The envelope is near thermal equilibrium at the beginning of the S–C transition, at $q_{c0} \lesssim 0.03$, and after it, at $q_{c0} \geq 0.11$, when it approaches the giant branch. However, the star is out of thermal equilibrium during that transition.

The last two panels in Fig. 3 zoom into the range around the core boundary for $q_{c0} = 0.00$ and $q_{c0} = 0.03$. The arrows show the locations of the core boundary according to the different definitions of q_c . In our opinion, the most physically justifiable definition is that corresponding to the location of the surface separating the contracting inner part of the core from the expanding outer layers, i.e., q_{c1} .

We then show in Fig. 4 the time dependence of the effective temperature, T_e , around the S–C transition for a $5M_{\odot}$ star. At the time of the central H exhaustion, $q_{c0} = 0$, but there is already a He-dominated core with $X \ll 1$, and $X = 0.01$ is reached only at $M_r/M = 0.076$. At $q_{c0} = 0.03$, q_c defined by the transition from collapse to expansion and by $X = 0.01$ is already about twice and thrice as high, respectively. The acceleration of the evolution of the effective temperature starts around this point, and the rate of the decrease of T_e keeps increasing up to $q_{c0} \approx 0.11$, which corresponds to the transition to the giant branch. Thus, the S–C phenomenon can be described as a quite extended phase in q_{c0} , from 0.03 to 0.11, but it is much more rapid in terms of q_{c1} , or even more so of q_{c2} , from about 0.09 to 0.12. Still, the phenomenon is more a smooth transition than a sharp limit.

The red curve in Fig. 4 shows the behaviour of a $5M_{\odot}$ configuration for which strict thermal equilibrium is enforced (no gravitational energy release or consumption and strict isothermality of the core). This sequence ends at the fractional core mass corresponding to $q_{c0} \approx 0.036$, $q_{c1} \approx 0.070$ and $q_{c2} \approx 0.087$. This case illustrates the classical assumption used to derive the S–C limit, where there are models satisfying this assumption only below the limit. However, real stars do not behave this way, and follow the sequence shown by the green curve. Along it, the process of the departure from the thermal equilibrium initially accelerates then later decelerates but is always gradual. It is then difficult to single out a specific fractional core mass and define it as the S–C limit.

Fig. 5 shows the distributions of the interior temperature as functions of the mass enclosed for stars of $M = 1.4$ and $6M_{\odot}$ and for different q_{c0} . We see that the He cores lose their isothermality and thus start to contract soon after the central hydrogen exhaustion. Initially this contraction is relatively slow. For $q_{c0} = 0.03$, the core remains approximately isothermal. Then, the contraction accelerates, and when the core approaches the expected S–C limit ($q_{c0} \approx 0.1$), it is already very far from being isothermal. Thus, the basic assumption used in deriving the S–C limit is not satisfied. We also see the expected return to isothermality for larger cores at $1.4M_{\odot}$ because the core becomes degenerate.

We have also found an interesting and unexpected behaviour of the radius of the star, namely first a local decrease then a local increase, see Fig. 6. We have found this phenomenon always at the fractional mass of the He core of $q_{c0} \approx 0.1$, i.e., around the end of the S–C transition, and for the mass range of 1.4 to $7M_{\odot}$, where

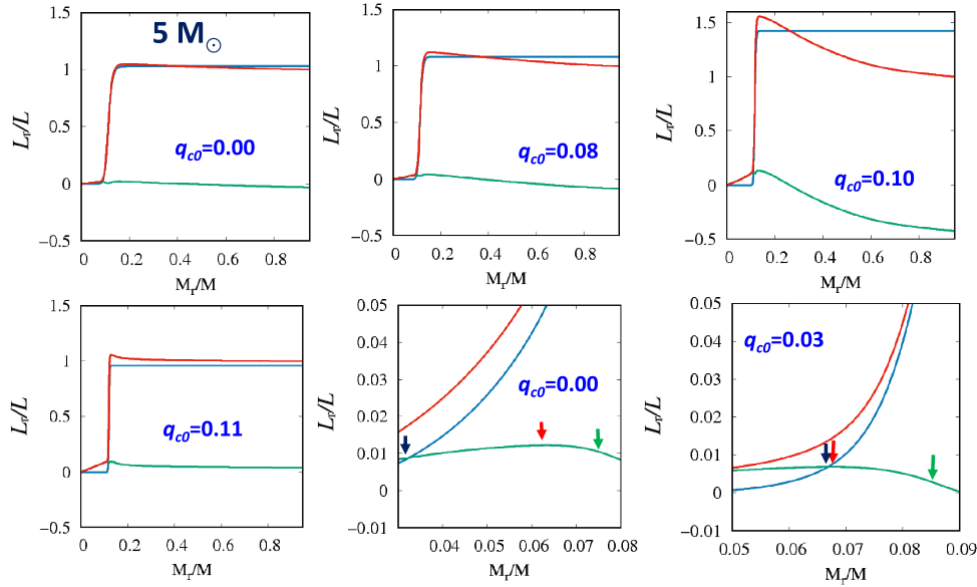


Figure 3. The local luminosity (i.e., the total energy flux through the surface of a sphere of a given radius), L_r , vs. the corresponding enclosed mass for a $5M_{\odot}$ star and for different values of q_{c0} . We plot L_r/L , where L is the total surface luminosity of the star, in terms of M_r/M . The green curves show the gravitational energy flux (positive when generated by core contraction and negative by envelope expansion). The blue curves show the flux generated by the nuclear reactions (H shell burning). The red curves show the sum. We see that after the central H exhaustion, the star gradually departs from the thermal equilibrium and later returns to it when approaching the giant branch. The last two panels zoom to the area near the core boundary for the cases of $q_{c0} = 0.00$ and 0.03 . The dark blue arrows show the location where the nuclear and gravitational energy fluxes are equal. The red arrows indicate the surface separating the contracting inner part of the core from the expanding outer layers. The green arrows indicate the surface with $X = 0.01$.

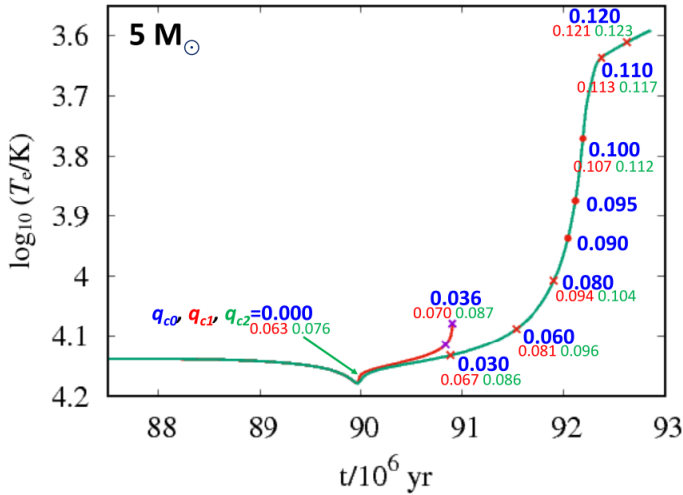


Figure 4. The green curve shows the stellar effective temperature vs. the evolutionary time (from the zero-age main sequence) for a $5M_{\odot}$ star. The values of q_{c0} (negligible H), q_{c1} (at the radius at which the core ceases to collapse) and q_{c2} ($X \leq 0.01$) are shown along the track. The left edge of the plot corresponds to the first turn on the H–R diagram, at which the central H content is about 0.05. The point with $q_{c0} = 0$ corresponds to the second turn on the H–R diagram and the time of the central H exhaustion. For comparison, the red curve shows a case when the strict thermal equilibrium is enforced (no gravitational energy release and isothermality of the core). This sequence ends at $q_{c1} \approx 0.070$, $q_{c2} \approx 0.087$. While these correspond to the classical S–C limit, this case is artificial.

this phenomenon takes place. The black crosses in Fig. 1 mark the points at which the radius as a function of time, $R(t)$, executes the

wiggle shown in Fig. 6, starting to increase again after a temporary decrease.

The values of q_{c0} for which this happens increase rather slowly with M , 0.090 for $M = 1.4M_{\odot}$, 0.098 for $4M_{\odot}$, 0.109 for $6M_{\odot}$ and 0.114 for $7M_{\odot}$, i.e., in the narrow range of q_{c0} of 0.09–0.11. This narrowness is surprising, taking into account large spans of other parameters of the stars at this phase of the evolution. For example, we have the radius of $R = 2.76R_{\odot}$ and the central temperature of 3.0×10^7 K for $M = 1.4M_{\odot}$ and $54.8R_{\odot}$, 1.0×10^8 K for $7M_{\odot}$. Thus, this phenomenon appears to be caused in some way by the core collapse, but details remain unclear. In Fig. 1, we also see that the kink in $R(t)$ approximately coincides with the star moving from the subgiant branch of into red giant branch. (We use here the terms subgiant and red giant in the sense of the location in the H–R diagram.) We note that changes in the character of the time dependence occur only for the stellar radius. The luminosity evolution does not show any features, and it monotonically decreases through the evolutionary phase of interest.

Coming back to Fig. 4, we see that the rate of the evolution (as measured by the changing effective temperature; the changes of L are even slower, see Fig. 1) after the central H exhaustion remains rather slow for some time while the star has already quite an extended core composed mostly of helium. In the considered case of $5M_{\odot}$, there is a zone of avoidance (the Hertzsprung gap) for $3.7 \lesssim \log_{10}(T_e/K) \lesssim 4.0$, but subgiants with higher T_e move through that phase relatively slowly. An analogous situation, with a somewhat different range of the gap, occurs for other stellar masses. Thus, evolved stars are common on both sides of the gap.

On the other hand, King (1993) placed a limit on the mass of the donor in the binary V404 Cygni by arguing that the mass of its core has to be above the S–C limit because otherwise the star would not have left the main sequence. However, the S–C limit occurs quite some time after leaving the main sequence. One could

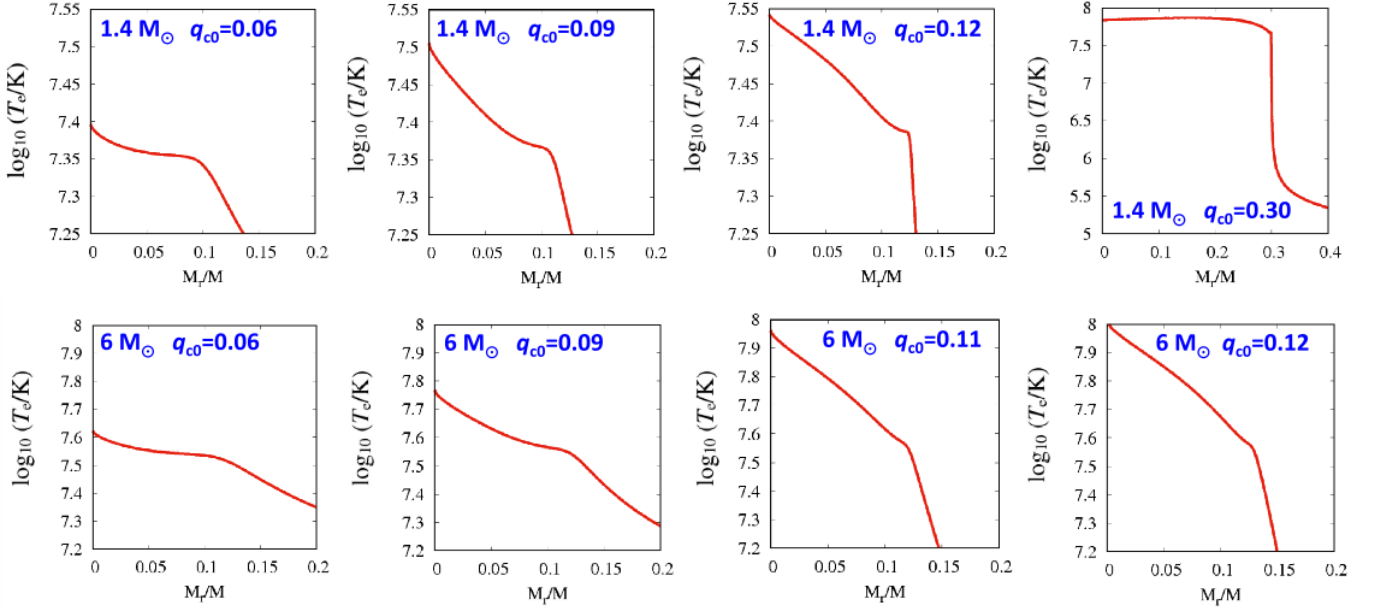


Figure 5. The interior temperature as functions of the mass enclosed for $M = 1.4$ and $6M_{\odot}$ and for different fractional core masses (with its strictest definition q_{c0}). We see the core loses isothermality (and thus starts to collapse) relatively quickly, at $q_{c0} \geq 0.06$. At the expected S–C limit, $q_{c0} = 0.1$, it is already far from isothermal. On the other hand, the core becomes isothermal again for $1.4M_{\odot}$ and $q_{c0} = 0.30$ because electrons become degenerate.

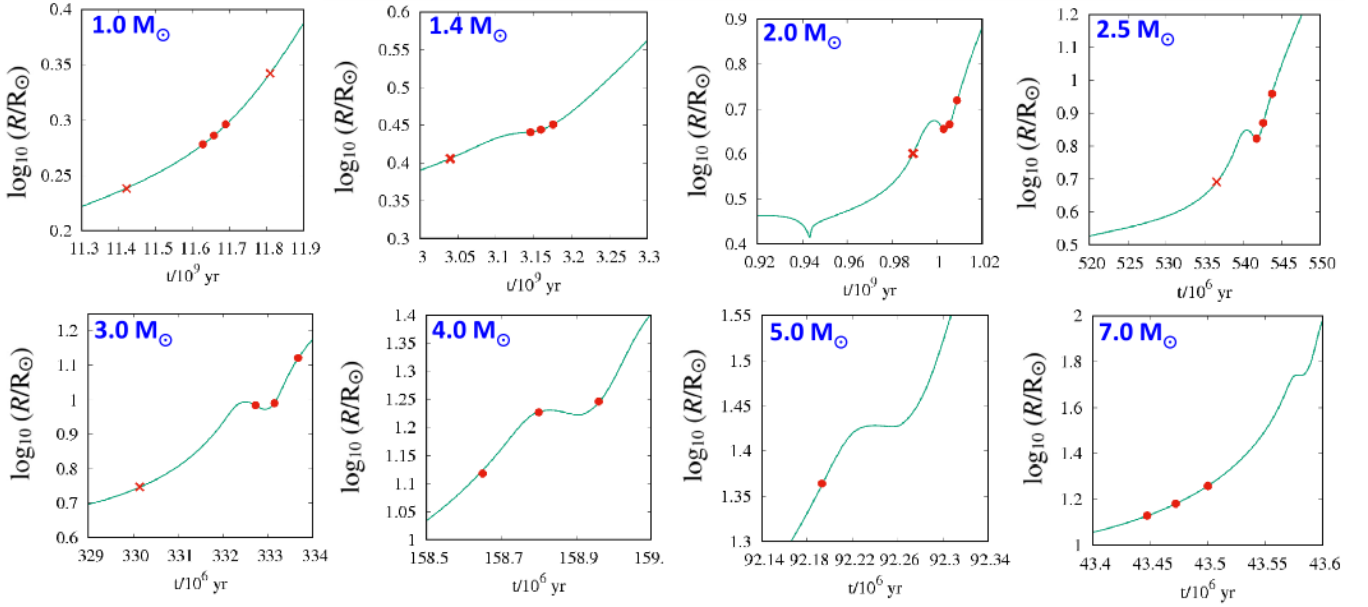


Figure 6. The stellar radius vs. the evolutionary time (from the zero-age main sequence) for $1 \leq M/M_{\odot} \leq 7$ stars. The red dots show the points where $q_{c0} = 0.09, 0.095$ and 0.1 (from left to right), and the red crosses show the points where $q_{c0} = 0.06$ (left) and 0.12 (right). The single red dot for $M = 5M_{\odot}$ star corresponds to $q_{c0} = 0.1$. The kinks in the shape of $R(t)$, i.e., at $dR/dt = 0$, occur close to $q_{c0} = 0.1$. They are present for $1.4 \leq M/M_{\odot} \leq 7$. The lower kink in $R(t)$ for $2M_{\odot}$ corresponds to the time of the central hydrogen exhaustion, $q_{c0} = 0$.

rather talk about the transition from a subgiant to giant, or from the luminosity class IV to III. The argument of King (1993) was then used by Muñoz-Darias, Casares & Martínez-Pais (2008) to constrain the donor mass in the binary GX 339–4. Subsequently, Heida et al. (2017) used the constraint of Muñoz-Darias et al. (2008) to place a strict upper limit on the mass of the black hole and a lower limit on the inclination of that binary. These constraints have then been later widely used in papers on that binary, see a discussion in Zdziarski, Ziółkowski & Mikołajewska (2019). However, the two best-fitting

stellar templates found by Heida et al. (2017) were one of the luminosity class III (a giant) and one of the class IV (a subgiant). Thus, evolved stars on both sides of the S–C limit were found to fit their observational data. Furthermore, the claimed maximum donor masses for V404 Cyg and GX 339–4 are about $1.3M_{\odot}$ and about $1.1M_{\odot}$, respectively, where the S–C limit does not apply. We also note that the numerical value of the limit used by King (1993), 0.17, is significantly above the canonical value of about 0.10.

3 CONCLUSIONS

We have studied in detail the evolution of the stars in the 1 to 7 M_{\odot} mass range from the time of leaving the main sequence up to reaching the giant branch, with the goal of presenting a comprehensive description of the Schönberg–Chandrasekhar transition. This transition occurs in the 1.4 to 7 M_{\odot} mass range. An important issue, which has apparently received no attention in the literature, is the way the He core is defined. When using the strict definition of the core as the region with the He abundance is close to null (with the fractional core mass denoted as q_{c0}) the S–C transition does not correspond to a sharp limit but instead occurs in an extended range of the fractional core mass, of 0.03 to 0.11. The cause of this is a very gradual core contraction causing a correspondingly gradual loss of the core isothermality with the increasing core mass. On the other hand, when using less strict definitions allowing for some H abundance, e.g., q_{c1} defined by the radius at which the core stops its collapse, or q_{c2} defined by $X \leq 0.01$, the S–C transition is found to be sharper, at the fractional core mass of about 0.07 to 0.11 and 0.09 to 0.12 for the former and latter definition, respectively. Thus, we should call this phenomenon an S–C transition rather than a limit. Therefore, it is difficult to single out a fractional core mass and define it as the S–C limit.

In Fig. 2, we illustrated the problem of a precise definition of the core boundary by showing the distribution of the H abundance vs. the mass within a given radius. This figure shows that the H abundance increases very gradually at the beginning of the S–C transition. This increase becomes much sharper when the transition is completed. Similarly, the power generated within a given mass increases gradually at low core masses, as shown in Fig. 3. Fig. 4 then shows an example of the temporal evolution of the effective temperature, showing the fractional core mass according to our three adopted definitions. It illustrates our statement that the acceleration of the temporal evolution occurs very gradually when the strict core definition, q_{c0} , is adopted, while the acceleration is occurs much faster for the other two definitions. Fig. 5 shows that the interior temperature decreases gradually even before the beginning of the S–C transition (whereas isothermality was the basic assumption made in the original derivation of the S–C limit).

For comparison, Fig. 4 also shows the behaviour of a 5 M_{\odot} configuration for which a strict thermal equilibrium was enforced (no gravitational energy release or consumption and a strictly isothermal core). In this case, in which the assumptions made in the derivation of the S–C limit are fully satisfied, we indeed find unambiguously the existence of a sharp S–C limit. Namely, we obtain models before reaching this limit, for which the fractional core mass is 0.070 or 0.087, depending on the definition, while there are no models satisfying our adopted assumptions above the limit. However, this case does not correspond to real stars.

We have also searched for a specific signature of the transit of the S–C limit, and found one. Namely, the stellar radius shows a wiggle at that transition, first decreasing and then increasing, as shown in Fig. 6.

We have also considered whether the S–C limit can be used as a diagnostic to constrain the evolutionary status of accreting X-ray binaries, but we have found such uses to be unfounded. The S–C limit does approximately correspond to the boundary between the subgiant and giant branches in the mass range of 1.4 to 7 M_{\odot} . However, in the specific cases when it was used in the past, the giant/subgiant distinction could not be made observationally and the claimed limiting stellar masses were less than 1.4 M_{\odot} .

ACKNOWLEDGEMENTS

We thank the anonymous first referee for a valuable report on the original version of this work, and the second referee, Prof. Christopher Tout, for a very careful analysis of the revised version. This research has been supported in part by the Polish National Science Centre under the grants 2015/18/A/ST9/00746 and 2019/35/B/ST9/03944.

DATA AVAILABILITY

There are no new data associated with this article.

REFERENCES

- Beech M., 1988, *Ap&SS*, 147, 219
 Cox J. P., Giuli R. T., 1968, *Principles of Stellar Structure*. Gordon and Breach, New York
 Eggleton P. P., Faulkner J., 1981, in Iben I., Renzini A., eds., *Physical Processes in Red Giants*. Reidel, Dordrecht, p. 179
 Eggleton P. P., Faulkner J., Cannon R. C., 1998, *MNRAS*, 298, 831
 Gamov G., 1938, *ApJ*, 87, 206
 Hayashi C., Hoshi R., Sugimoto D., 1962, *Prog. Theor. Phys. Suppl.*, 22, 1
 Heida M., Jonker P. G., Torres M. A. P., Chiavassa A., 2017, *ApJ*, 846, 132
 Henrich L. R., Chandrasekhar S., 1941, *ApJ*, 94, 525
 King A. R., 1993, *MNRAS*, 260, L5
 Kippenhahn R., Weigert A., Weiss A., 2012, *Stellar Structure and Evolution*. Springer-Verlag, Berlin Heidelberg
 Muñoz-Darias T., Casares J., Martínez-Pais I. G., 2008, *MNRAS*, 385, 2205
 Paczyński B., 1969, *Acta Astron.*, 19, 1
 Paczyński B., 1970, *Acta Astron.*, 20, 47
 Pamyatnykh A. A., Dziembowski W. A., Handler G., Pikał H., 1998, *A&A*, 333, 141
 Roth M. L., 1973, PhD thesis, University of Hamburg, unpublished
 Schönberg M., Chandrasekhar S., 1942, *ApJ*, 96, 161
 Zdziarski A. A., Ziółkowski J., Bozzo E., Pjanka P., 2016, *A&A*, 595, A52
 Zdziarski A. A., Ziółkowski J., Mikołajewska J., 2019, *MNRAS*, 488, 1026
 Ziółkowski J., 2005, *MNRAS*, 358, 851